



**HAL**  
open science

## The Pyrenees: glacial landforms from the Younger Dryas (12.9–11.7 ka)

Magali Delmas, Marc Oliva, Yanni Gunnell, Théo Reixach, Marcelo Fernandes, José Fernández-Fernández, Marc Calvet

### ► To cite this version:

Magali Delmas, Marc Oliva, Yanni Gunnell, Théo Reixach, Marcelo Fernandes, et al.. The Pyrenees: glacial landforms from the Younger Dryas (12.9–11.7 ka). *European Glacial Landscapes*, Elsevier, pp.541-552, 2023, 978-0-12-823498-3. 10.1016/B978-0-323-91899-2.00038-3 . hal-03989979

**HAL Id: hal-03989979**

**<https://univ-perp.hal.science/hal-03989979>**

Submitted on 28 Apr 2023

**HAL** is a multi-disciplinary open access archive for the deposit and dissemination of scientific research documents, whether they are published or not. The documents may come from teaching and research institutions in France or abroad, or from public or private research centers.

L'archive ouverte pluridisciplinaire **HAL**, est destinée au dépôt et à la diffusion de documents scientifiques de niveau recherche, publiés ou non, émanant des établissements d'enseignement et de recherche français ou étrangers, des laboratoires publics ou privés.

## **PART IV. European glacial landforms from the Younger Dryas (12.9–11.7 ka)**

### **SECTION 2 European regions that were not covered by the EISC**

**Abstract:** As elsewhere around the North Atlantic, and throughout most European mountains, the Younger Dryas (YD: 12.9–11.7 ka) corresponded in the Pyrenees to a short period of cold climate, less intense than at the time of the Oldest Dryas (~18.9–14.6 ka) but notably colder than at the time of the Bølling–Allerød Interstadial (14.6–12.9 ka). The response of Pyrenean glaciers to the YD cold spike has been documented in just ten sites, mostly by  $^{10}\text{Be}$  and  $^{36}\text{Cl}$  exposure ages obtained from glacially-polished bedrock steps on valley floors, with only a few exposure ages from moraines and rock glaciers. Despite some uncertainty over age precision (mainly ascribable to uncertainty concerning past snow cover), all existing evidence indicates that YD glaciers, where present, prevailed mostly in the central and western Pyrenees and never exceeded lengths of 2–6 km. Ongoing deglaciation favoured paraglacial readjustments on cirque headwalls, promoting the widespread development of rock glaciers and, more locally, debris-covered glaciers.

**Key words:** Younger Dryas stadial moraine, terrestrial cosmogenic nuclide exposure dating, climatic gradient, Pyrenees

#### **56. The Pyrenees: glacial landforms from the Younger Dryas**

(Magali Delmas, Marc Oliva, Yanni Gunnell, Théo Reixach, Marcelo Fernandes, José M. Fernández-Fernández and Marc Calvet)

##### **56.1. Climatic and environmental conditions during the Younger Dryas**

As elsewhere around the North Atlantic region (Naughton et al., 2022), and throughout most European mountains (García-Ruiz et al., 2022), the Younger Dryas (hereafter YD, i.e., GS-1 after Rasmussen et al., 2014) in the Pyrenees corresponds to a short period of cold climate, less intense than at the time of the Oldest Dryas (hereafter OD, or early last glacial-to-interglacial transition, LGIT: 18.9–14.6 ka) but notably colder than at the time of the Bølling–Allerød Interstadial (hereafter B-A, i.e., GI-1: 14.6–12.9 ka after Rasmussen et al., 2014). For example, in the central Pyrenees summer air palaeotemperatures during the YD, inferred from chironomids in the lacustrine sediment sequence at Ech palaeolake (710 m), were estimated to lie around 15–15.5 °C, as opposed to 10 to 13 °C during the OD, but between 16 and 17.5 °C during the first part of the B-A and ~17 °C at the beginning of the Holocene (Millet et al., 2012; see Fig. 56.1 for location). In NW Iberia, similar data from Laguna de la Roya (1608 m) document summer palaeotemperatures of ~10 °C during the YD, against 7–8 °C during the OD and 12–13 °C during the B-A (Muñoz Sobrino et al., 2012). On the western side of the Pyrenees, stalagmites from Ostolo cave (248 m a.s.l., Basque mountains) record a cooling in mean annual temperature of ~5 °C between 12.9 and 12.8 ka (model age based on 61 U–Th data points) inferred from a decrease of 1.6 ‰ in  $\delta^{18}\text{O}$  values (Bernal-Wormull et al., 2021). Similar magnitudes of cooling are also reported in the central Pyrenees based on the high-resolution  $\delta^{18}\text{O}$  record from Seso cave (794 m, Ara valley; Bartolomé et al., 2015). Moreover,  $\delta^{18}\text{O}$  values recorded at Ostolo cave during GS-2.1a (–7 to –9‰) are substantially lower than at the time of GS-1 (6‰), suggesting a climate colder at the time of GS-2.1a (17.5–14.6 ka) than of GS-1 (Bernal-Wormull et al., 2021). These trends concur with SST values recorded in the Alboran Sea and the Gulf of Lion during the Last Glacial-to-Interglacial Transition (LGIT; Cacho et al., 1999, 2001, 2002; Melki et al., 2009; Rodrigues et al., 2010).

In terms of moisture regime, the stalagmite from Seso Cave reveals the occurrence of two distinct periods within the YD: whereas the first (12.9–12.5 ka) was very cold and dry, as demonstrated by slow stalagmite growth rates and low isotope ratios ( $\delta^{18}\text{O}$ ,  $\delta^{13}\text{C}$ ) during that period, the second (12.5–11.7 ka) featured wetter conditions, probably triggered by an intensification of the thermohaline circulation in the Atlantic (Bartolomé et al., 2015). Along the northern edge of the Ebro Basin, the Estanya lacustrine sequence (670 m) records a peak of aridity during the YD, documented by a decrease in lake levels (near total absence of diatoms between 12.8 and 11.8 cal ka BP as a consequence of the low lake level and high alkalinity), an increase in salinity suggested by the sedimentation of gypsum-rich facies, and a sudden decline in organic productivity (Morellón et al., 2009). By contrast, the Estanya pollen spectra record a complex response to YD-related climate forcing, with an increase of semi-deciduous and evergreen oaks indicating the presence of mesothermophylous vegetation refugia near the site (Vegas-Villarrúbia et al., 2013), as elsewhere in the Ebro Basin (Gonzalez-Sampéris et al., 2004). In the rest of the Pyrenees, all studies record substantial land cover change in response to the cold and arid conditions that prevailed at the time of the YD (syntheses in Jalut et al., 1992; Fletcher et al., 2010; Moreno et al., 2012, 2014). Pollen spectra document a return of steppe taxa (*Juniperus*, *Artemisia*, *Chenopodiaceae*) as forest receded (decline in *Ephedra*, *Betula*, *Pinus*) to maximum elevations of ~1300 m, as opposed to ~1700 m at the time of the B-A (Reille and Andrieu, 1993).

Palaeoclimatic changes during the YD do not appear to have had a strong impact on stream behaviour, as already since the B-A Interstadial rivers were on a trajectory involving the abandonment of braided patterns and a decline in sediment loads favoured by hillslope stabilisation under the expansion of forest vegetation on mountainsides. The absence of YD palaeoenvironmental signatures in valleys could also, however, be explained by the low precision of geochronological constraints on the stratigraphic record of glaciofluvial deposits in the Pyrenean foothills (Stange et al., 2013, 2014; Delmas et al., 2015, 2018; Nivière et al., 2016; Mouchéné et al., 2017; synthesis in Delmas, 2019).

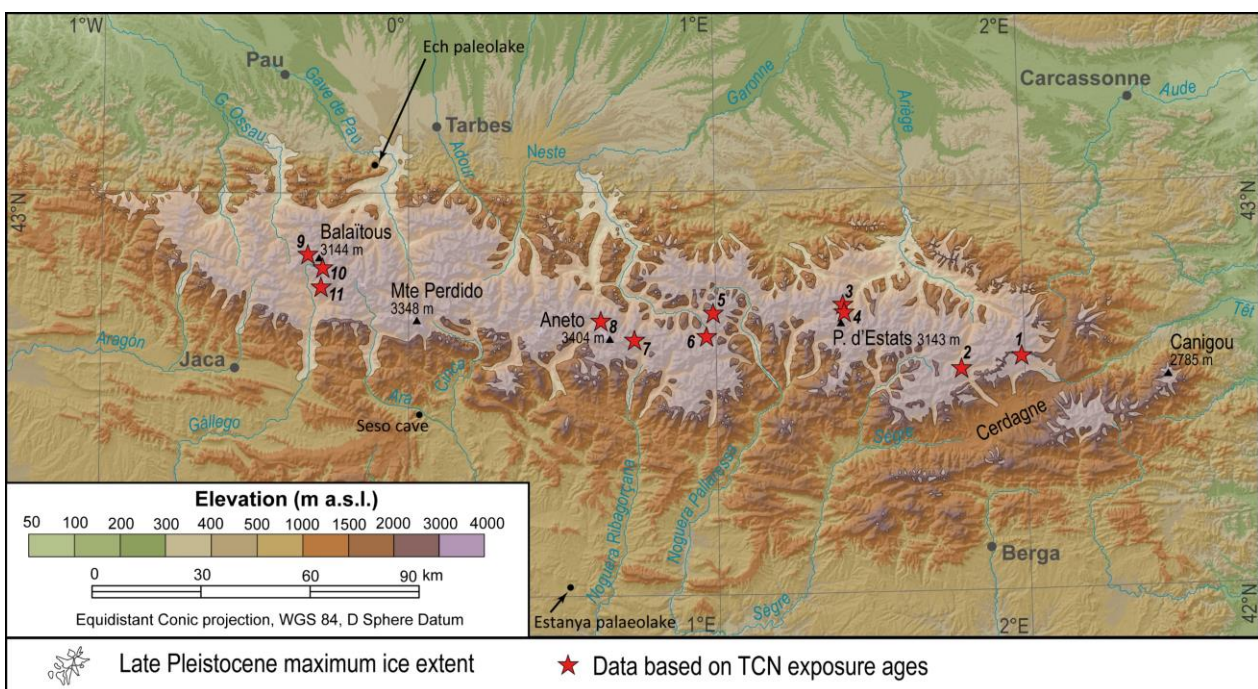


**Figure 56.1. Spatial distribution of published research on the Younger Dryas (12.9–11.7 ka) in the Pyrenees.** 1- Grave Cirque/upper Têt valley (Delmas et al., 2008; Reixach et al., 2021). 2- Orri Cirque/upper Querol valley (Pallàs et al., 2010; Reixach et al., 2021). 3- Bassiès Cirque/upper Vicdessos valley (Crest et al., 2017). 4- Médecourbe Cirque/upper Vicdessos valley (Jomelli et al., 2020; Reixach et

*al.*, 2021). 5- Bacivèr Cirque/upper Garonne valley (Oliva et al., 2021). 6- Ruda Cirque/upper Garonne valley (Fernandes et al., 2021). 7- Mulleres and Besiberri cirques/Noguera Ribagorçana valley (Pallàs et al., 2006). 8- Aneto and Maladeta cirques/Ésera valley (Crest et al., 2017). 9- Arrémoulit Cirque/upper Ossau valley (Palacios et al., 2017). 10- Piedrafita/upper Gállego valley (Palacios et al., 2015b, 2017). 11- Brazato, Piniecho and Catieras cirques/upper Gállego valley (Palacios et al., 2015b, 2017).

## 56.2. Record of glacier responses to colder and drier conditions

The response of Pyrenean glaciers to the YD cold spike has been documented in just a handful of valleys (Fig. 56.1, see syntheses in García-Ruiz et al., 2016; Oliva et al., 2019). Evidence is mostly based on  $^{10}\text{Be}$  and  $^{36}\text{Cl}$  exposure ages obtained from glacially-polished bedrock steps on valley floors, with only a few exposure ages from moraines and rock glaciers (Pallàs et al., 2006, 2010; Delmas et al., 2008, 2011; Palacios et al., 2015a, 2015b, 2017; Crest et al., 2017; Andrés et al., 2018; Jomelli et al., 2020; Oliva et al., 2021; Reixach et al., 2021; Fernandes et al., 2021). Despite uncertainty over exposure ages (mainly ascribable to uncertainties derived from snow-cover correction factors), all existing evidence indicates that YD glaciers were confined to the cirques and never exceeded lengths of 2–6 km — even in the central Pyrenees, where hypsometry in the most elevated massifs (> 3000 m) potentially offers the largest available ice accumulation areas.

### 56.2.1. Central Pyrenees

In the upper part of the Noguera Ribagorçana valley, previously published exposure ages were modelled without any correction for snow shielding because this variable is difficult to appreciate accurately at any given sampling site (Pallàs et al., 2006). By using revised age equation parameters (see method for standardising ages in Palacios et al., 2022), results reveal that moraines initially attributed to the early Holocene (Pallàs et al., 2006) now correlate with the B-A Interstadial (GI-1) or with the onset of the YD (GS-1), depending on whether or not a snow correction factor (SCF) is applied. The Mulleres frontal moraine (1720 m), for example, yielded a weighted mean age of  $13.0 \pm 0.1$  ka (MUL01, a boulder:  $13.0 \pm 2.1$  ka; and MUL04, an ice-polished bedrock step:  $13.0 \pm 1.4$  ka). For SCF = 0.97, values for this same site shift to  $13.5 \pm 2.2$  ka (MUL01) and  $13.6 \pm 1.5$  ka (MUL04), thereby raising the weighted mean age to  $13.5 \pm 0.1$  ka. In the same valley, moraines on cirque floors in the upper Besiberri (2700 m) and Pleta Naua (2200 m) yielded mean-weighted ages of  $12.6 \pm 0.1$  ka (sample LDB:  $12.5 \pm 1.2$  ka,  $12.7 \pm 1.1$  ka,  $12.7 \pm 1.2$  ka) and  $12.8 \pm 0.3$  ka (sample OPN:  $13.3 \pm 1.3$  ka,  $12.6 \pm 1.7$  ka,  $12.6 \pm 1.2$  ka), respectively. When applying SCF values of 0.84 and 0.91, these same two sites record mean weighted ages of  $14.9 \pm 0.1$  ka (LDB:  $14.8 \pm 1.4$  ka,  $15.1 \pm 1.2$  ka,  $14.8 \pm 1.3$  ka) and  $14.2 \pm 0.4$  ka (OPN:  $14.7 \pm 1.4$  ka,  $14.0 \pm 1.8$  ka,  $13.9 \pm 1.3$  ka). Overall, the data indicate that, either at the start of the YD or during the colder spikes of the B-A (such as the Older Dryas), the upper Noguera Ribagorçana valley hosted cirque glaciers of variable sizes depending on local characteristics, aspect and topography: e.g., a small, 4-km-long valley glacier on the SE flank of the Maladeta massif descending to ~1720 m (Mulleres) and associated with an equilibrium-line altitude (ELA) around 2450 m; and cirque glaciers < 1 km long, such as at Pleta de Nau (glacier front at 2200 m) and in the upper Besiberri catchment (front at 2700 m).

On the northern face of the Maladeta massif, the Renclusa and Aigualluts moraines represent two local stadial positions below the LIA (Little Ice Age) moraines (Fig. 56.2). During the Renclusa stade, the Aneto and Maladeta glaciers were 2.8 km long and 2.6 km long, respectively, each descending to 2265 m and 2280 m. The ELA estimated from these two cirque glaciers was established at ca. 2800 m. During the Aigualluts stade, the Aneto and Barrencs cirques were hosting a 4.7-km-long glacier (front positioned around 2010 m), while the Maladeta glacier attained a length of 3.5 km (front around 1965 m). On that

basis, the ELA had fallen to 2640 m. By comparison, Aneto Cirque during the LIA hosted a glacier 2.5 km long (front ~2475 m), while its Maladeta counterpart was merely 1.6 km long (front ~2605 m), with a corresponding ELA around 2970 m. Exposure ages obtained for those two stadal moraines are quite scattered (Crest et al., 2017), but they can be ascribed to the YD and OD, respectively, mainly on the basis of the oldest age obtained for boulders on the Aigualluts moraine (Fig. 56.2). Such an interpretation of the age data for the Renclusa and Aigualluts moraines implies sharp local contrasts in ELA positions given that values of 2450 m during the B-A and YD on the SE face of the Maladeta massif (Mulleres, Table 56.1) occurred concurrently with ELA values of 2800 m during the YD on its north face (Renclusa). An alternative to this potentially implausible discrepancy lies in considering that the north-facing Renclusa and Aigualluts stadal moraines are younger than initially believed, and thus are of YD or early Holocene age. Ongoing surface exposure dating should hopefully contribute to clarify these issues.

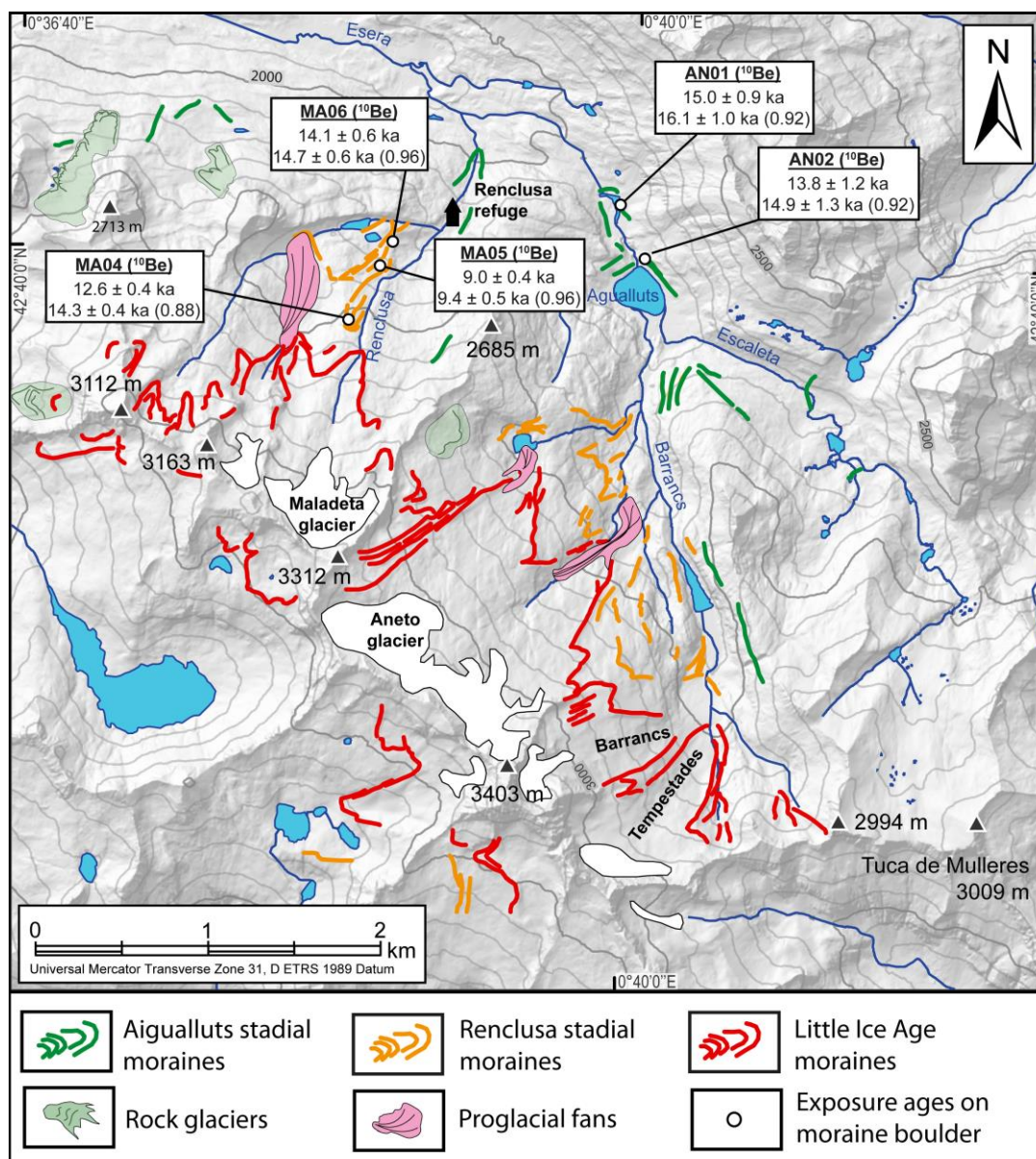


**Figure 56.2. Glacial and proglacial deposits, with associated ages, in the upper Ésera (Aneto–Maladeta massif).** Note that each exposure age is reported without (top) and with (bottom) a snow correction factor (SCF values indicated in brackets). Digital elevation data source: Instituto Geográfico Nacional; ground resolution: 5 m.

In the Ruda valley (Val d’Aran/Garonne valley), a  $13.0 \pm 0.8$  ka moraine suggests the existence of a 3-km-long glacier at the time of the B-A/YD transition. Moreover, glacially-polished surfaces from the highest part of the valley in Saboredo Cirque provided ages of  $12.7 \pm 0.7$  ka, similar to ages obtained from a local cirque moraine ( $12.6 \pm 1.3$  ka; Fernandes et al., 2011) as well as from another nearby, in Bacivèr Cirque ( $12.8 \pm 0.5$  ka; Oliva et al., 2021). Overall, the age ranges obtained indicate the existence of glaciers during the early YD, persisting only in the highest and more sheltered parts of the Garonne valley.

**Table 56.1. Glaciers in the Pyrenees during the Younger Dryas (12.9–11.7 ka)**

| Valley name<br>(glacier name) | Glacier<br>front<br>elevation<br><br>(m) | Glacier<br>length<br><br>(km) | ELA                        |                              |                               | Age of late LGIT deposits<br><br>(ka $\pm$ 1 $\sigma$ )   | Key<br>references               |
|-------------------------------|--|-------------------------------|----------------------------|------------------------------|-------------------------------|---|---------------------------------|
|                               |  |                               | THAR <sup>1</sup><br>(m)   | AAR <sup>5</sup><br>(m)      | AABR <sup>10</sup><br>(m)     |   |                                 |
| N. Ribagorçana<br>(Mulleres)  | 1720                                     | 3                             | 2370–<br>2490 <sup>2</sup> | 2321 $\pm$<br>50             | 2371 $\pm$ 50                 | 13.0 $\pm$ 0.1 ka ( <sup>10</sup> Be exposure ages from one boulder on the Mulleres frontal moraine and one polished bedrock surface near Mulleres moraine)                               | Pallàs et al.,<br>2006          |
| N. Ribagorçana<br>(Mulleres)  | 1720                                     | 3                             |                            | 2450 <sup>6</sup>            |                               | Idem  |                                 |
| Ésera<br>(Aigualluts)         | 2010                                     | 5–6                           | 2480–<br>2560 <sup>3</sup> | 2615 $\pm$<br>50             | 2665 $\pm$ 50                 | 16.2 $\pm$ 1.1 ka, 14.9 $\pm$ 1.3 ( <sup>10</sup> Be exposure ages from boulders, Aigualluts lateral moraine)<br>Younger exposure ages unpublished  | Crest et al.,<br>2017           |
| Ésera<br>(Renclusa)           | 2265                                     | 3                             | 2825–<br>2945 <sup>3</sup> | 2788 $\pm$<br>50             | 2800 $\pm$ 50                 | 14.3 $\pm$ 0.4 ka, 9.4 $\pm$ 0.5 ka, 14.1 $\pm$ 0.6 ka ( <sup>10</sup> Be exposure ages from boulders, Renclusa lateral moraine)<br>Younger exposure ages unpublished                     | Crest et al.,<br>2017           |
| Gállego<br>(Piniecho)         | 2350                                     | > 1                           | 2450–<br>2500 <sup>4</sup> | -                            | -                             | <sup>36</sup> Cl and <sup>10</sup> Be exposure ages (n = 12) from boulders on cirque glacier moraines and on rock glaciers  | Palacios et al., 2015b,<br>2017 |
| Val D’Aran<br>(Ruda)          | 2470                                     | 0.4                           | -                          | 2568 -<br>10/+5 <sup>7</sup> | 2571 -<br>15/+5 <sup>11</sup> | 12.6 $\pm$ 1.3 ka (mean of <sup>10</sup> Be exposure ages from two moraine boulders) and 12.7 $\pm$ 0.8 ka (mean of <sup>10</sup> Be exposure ages from two samples in polished surfaces) | Fernandes et al., 2021          |
| Vicdessos<br>(Mouscadous)     | 1885                                     | 3.5                           |                            | 2200 <sup>8</sup>            |                               | 12.3 $\pm$ 0.2 ka (mean-weighted <sup>10</sup> Be exposure ages from 2 boulders on Mouscadous lateral moraine)  | Crest et al.,<br>2017           |
| Vicdessos<br>(Médecourbe)     | 2230                                     | 1.6                           |                            | 2525 <sup>9</sup>            |                               | 13.2 $\pm$ 0.9 ka (mean weighted <sup>10</sup> Be exposure ages from 4 boulders on Médecourbe frontal moraine)  | Jomelli et al.,<br>2020         |

<sup>1</sup> ELA calculated using the toe-to-headwall altitude ratio (THAR) method (ratio of 0.6).

<sup>2</sup> Data calculated for ridgetop elevations of 2800 and 3000 m, respectively.

<sup>3</sup> Data calculated for ridgetop elevations of 3200 and 3400 m, respectively.

<sup>4</sup> Data calculated for ridgetop elevations of 2500 and 2600 m, respectively.

<sup>5</sup> ELA calculated using the accumulation area ratio (AAR) method (ratio of 0.65  $\pm$  0.05).

<sup>6</sup> Value for the reconstructed glacier based on Harper and Humphrey (2003) and using the Mulleres frontal moraine as the glacier boundary.

<sup>7</sup> A balance ratio of 0.6  $\pm$  0.05 was used for the AAR method.

<sup>8</sup> Value for the reconstructed glacier based on Harper and Humphrey (2003) and using the Mouscadous lateral moraine as the glacier boundary.

<sup>9</sup> Value for the reconstructed glacier based on Harper and Humphrey (2003) and using the Médecourbe frontal moraine as the glacier boundary.

<sup>10</sup> ELA calculated using the area–altitude balance ratio (AABR) methods (balance ratio of 1.59; Rea, 2009).

<sup>11</sup> A balance ratio of 1.9  $\pm$  0.81 for the AABR method.

## 56.2.2. Western Pyrenees

In the upper valley of the Gave d'Ossau, three  $^{10}\text{Be}$  exposure ages (ARR-1:  $7.9 \pm 2.1$  ka, ARR-2:  $11.1 \pm 0.6$  ka; ARR-3:  $10.4 \pm 0.6$  ka) were obtained from glacially-polished rock surfaces on the floor of Arrémoulit Cirque (2300 m, below Pic Arriel, 2824 m; Palacios et al., 2017). Using SCFs of 0.93, 0.88, and 0.79, those three samples yield corrected ages of  $8.5 \pm 2.3$  ka,  $12.5 \pm 0.7$  ka and  $13.0 \pm 0.8$  ka, respectively (Fig. 56.3). They indicate that definitive deglaciation of this north-facing cirque occurred during the YD or the Early Holocene.

In the upper Gállego catchment (Aiguas Limpias valley), on the southern flank of Pic Balaitous (3145 m), five samples were collected from glacially-polished rock surfaces on cirque floors (RES-3, RES-4, RES-5, RES-6, RES-7, elevations between 2550 and 2750 m; Fig. 56.3). The  $^{36}\text{Cl}$  and  $^{10}\text{Be}$  exposure ages are very similar to those obtained from Arrémoulit and lead to the same conclusions.

A few kilometres to the SE, in the Caldarés valley headwater, one of the main tributaries of the Gállego catchment, 20 samples were collected from three cirques (Brazato, Piniecho and Catieras). They were obtained from a variety of large boulders on moraines or resting directly on a bedrock plinth, from rock-glacier boulders, as well as from ice-polished bedrock exposures (Fig. 56.4). These exposure ages show that all three glaciers were confined to their cirques during the YD, and only formed a very short valley glacier in one case. Results also show that the Brazato rock glacier developed at the beginning of the Holocene and remained active until the Holocene Thermal Maximum because of the protective effect of large masses of blocks and boulders (Palacios et al., 2015b, 2017).

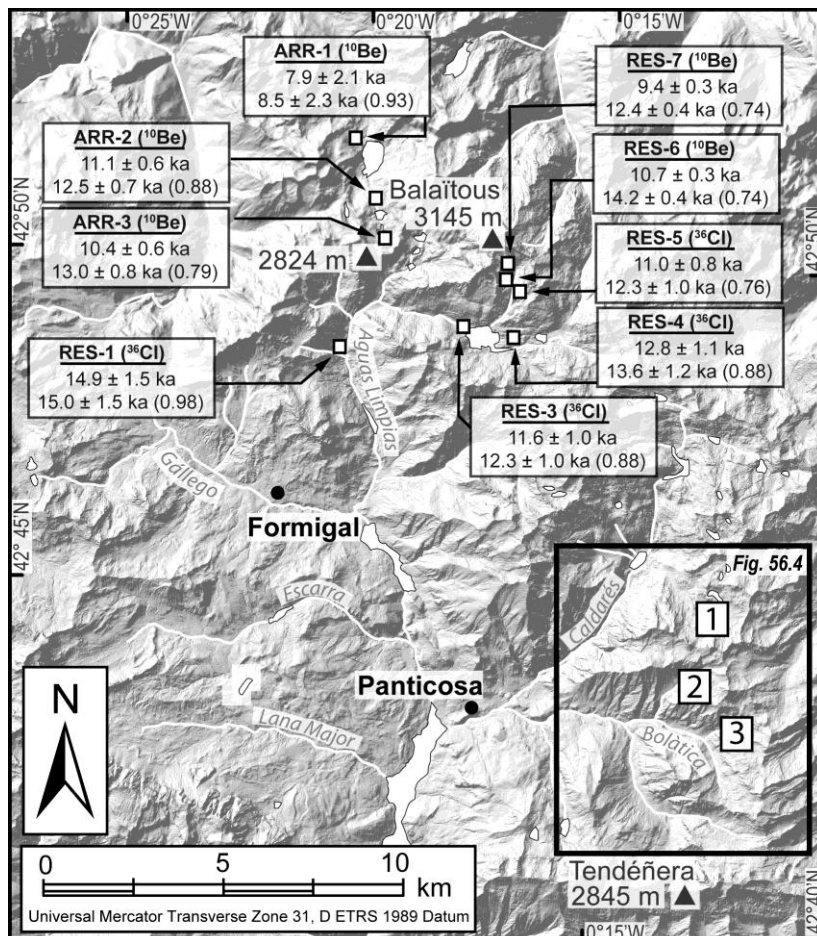


**Figure 56.3. Exposure ages in the Arrémoulit and Piedrafita cirque areas, Gállego catchment. 1- Brazato Cirque. 2- Piniecho Cirque. 3- Catieras Cirque. Note that each sample exposure age is reported without (top) and with (bottom) a snow correction factor (SCF values indicated in brackets). Digital elevation data source: Instituto Geográfico Nacional; ground resolution: 5 m.**

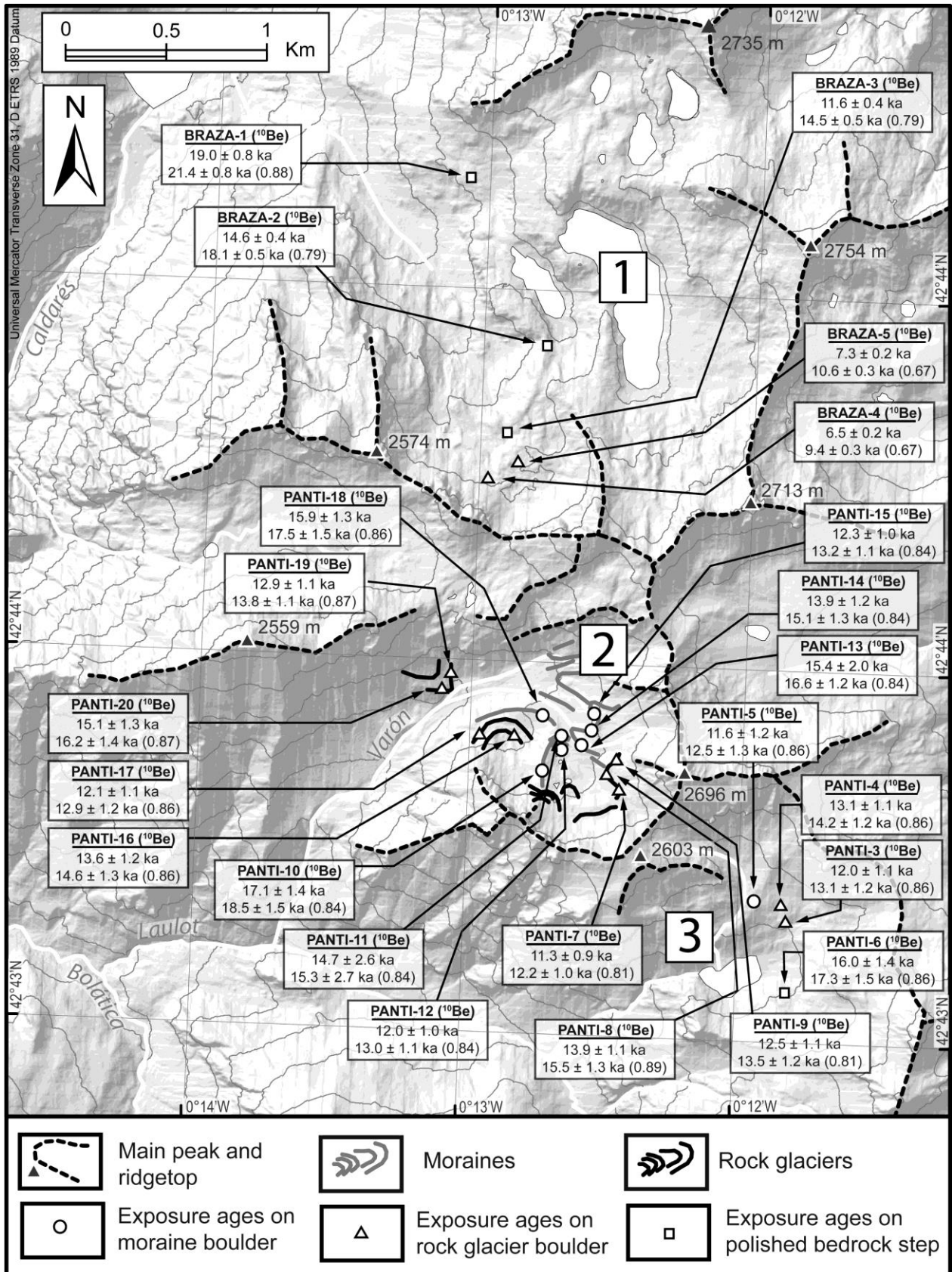


**Figure 56.4. Exposure ages in the Piniecho and Catieras cirques, Gállego catchment.** Base map (deposits, landforms and exposure ages) after Palacios et al. (2015b, 2017). 1- Brazato Cirque. 2- Piniecho Cirque. 3- Catieras Cirque. Note that each exposure age is reported without (top) and with (bottom) a snow correction factor (SCF values indicated in brackets). Digital elevation data source: Instituto Geográfico Nacional; ground resolution: 5 m.

### 56.2.3. Eastern Pyrenees

In the upper Vicdessos valley, ice-marginal deposits preserved in Bassiès Cirque have been helpful in reconstructing palaeoglacier geometries during two stadial stillstands (Légunabens stade, and Mouscadous stade) that correlate with the YD in the first case, and with the YD or the early Holocene in the second, depending on whether or not corrections for snow shielding are applied (Fig. 56.5; Crest et al., 2017, results remodelled by Reixach et al., 2021). At the time of the Légunabens stade (GS-2.1a), a glacier 6.5 km long and 150 m thick was hosted by the Escale valley and formed a diffidence lobe over the Col de Légunabens (a frontal moraine lying at 1500 m, coaxial with the diffidence, documents this scenario). On that basis, Reixach et al. (2021) modelled an ELA positioned at 2012 m, a mass-balance gradient of  $0.44 \pm 0.05 \text{ m}\cdot\text{yr}^{-1}\cdot 100 \text{ m}^{-1}$ , and best-fitting deviations from present-day reference conditions of  $-45 \pm 11\%$  for palaeoprecipitation (hereafter: P), and  $-9.1 \pm 0.5 \text{ }^\circ\text{C}$  for palaeotemperature (hereafter: T). At the time of the Mouscadous stade, the glacier had receded to the cirques. A lateral moraine located around 1885 m outlines the margin of a 3.5-km-long glacier, 70 m thick and with its tip reaching the 1660 m elevation contour. Reconstructed palaeoglaciological and palaeoclimatic conditions indicate an ELA at 2203 m, a mass-balance gradient of  $0.52 \pm 0.09 \text{ m}\cdot\text{yr}^{-1}\cdot 100 \text{ m}^{-1}$ , and best-fitting P and T pairs of  $-21 \pm 16\%$  and  $-7.0 \pm 0.5 \text{ }^\circ\text{C}$  (Reixach et al., 2021). As a result of temperature and precipitation rising by  $\sim +2 \text{ }^\circ\text{C}$  and  $\sim +20\%$  (Reixach et al., 2021), the ELA between the Légunabens and Mouscadous stadial moraines rose by 200 m during the YD/early Holocene. The inference for the eastern Pyrenees, therefore, is that climatic conditions at higher elevations were substantially milder at that time than earlier during the LGIT (e.g., during GS-2.1a, see Delmas et al., 2022a).

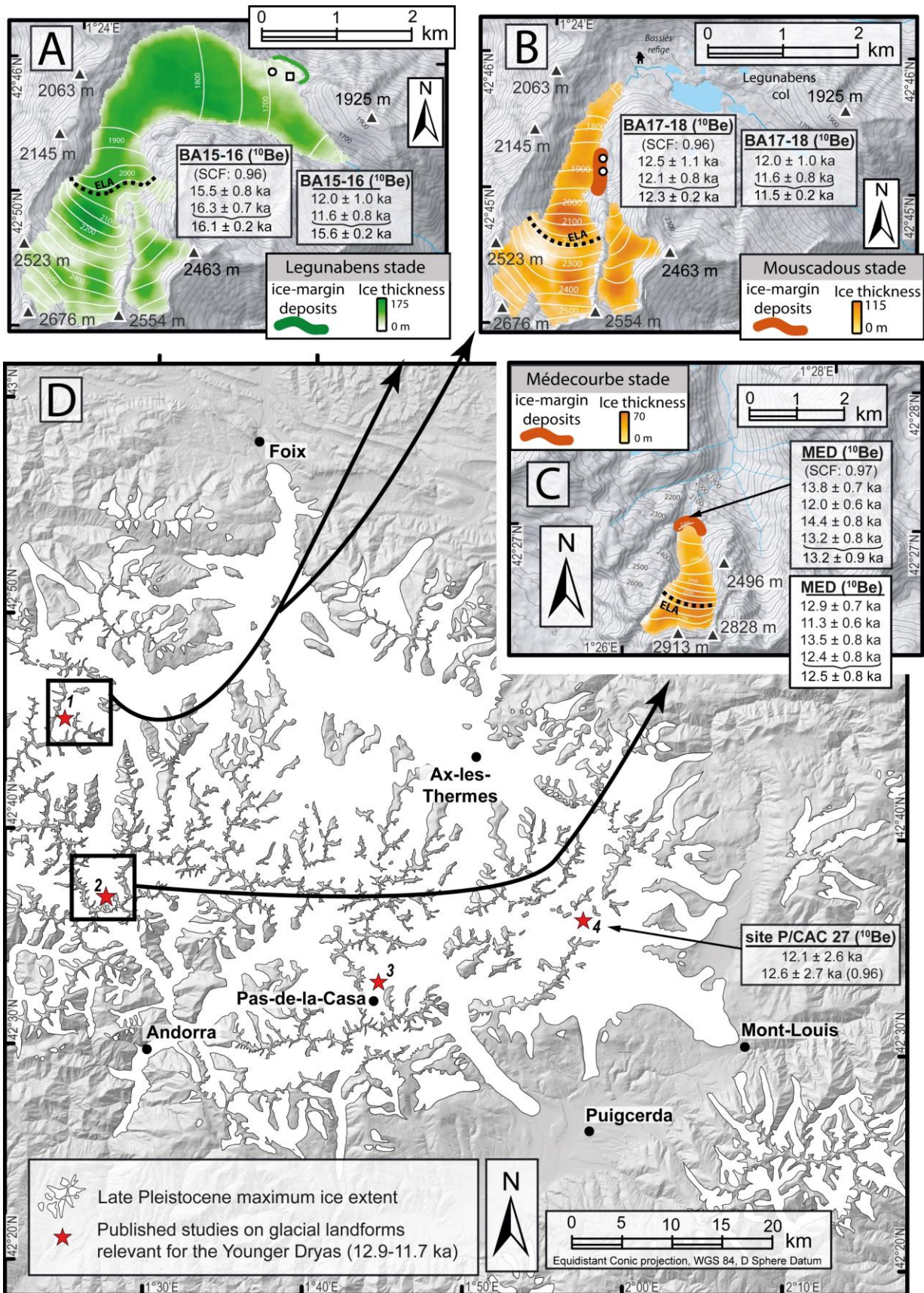


**Figure 56.5. Ice extent in the eastern Pyrenees during the Younger Dryas (12.9–11.7 ka).** A. Ice extent in Bassiès massif at the time of the GS-2.1a. B. Ice extent in Bassiès massif at the time of the YD or early Holocene. C. Ice extent in Medecourbe Cirque at the time of the B-A or YD. D. Location map. Red stars locate <sup>10</sup>Be and <sup>36</sup>Cl sampling sites: 1- Bassiès Cirque/upper Videssos valley (Crest et al., 2017; ages

*remodelled after Reixach et al., 2021). 2- Médecourbe Cirque/upper Vicdessos valley (Jomelli et al., 2017; ages remodeled after Reixach et al., 2021). 3- Pas de la Casa Cirque/ upper Ariège valley (possible YD glacier based on regional ELA, no exposure ages). 4- Grave Cirque/upper Têt valley (Delmas et al., 2008; ages remodelled after Reixach et al., 2021). For each sample in A, B and C, exposure ages with and without a snow correction factor (SCF values indicated in brackets) are presented in separate boxes, with weighted mean ages displayed below the curly bracket. In D, the sample exposure ages are reported without (top) and with (bottom) a snow correction factor (SCF value indicated in brackets).*

Further up the Vicdessos valley, boulders on the frontal moraines of Médecourbe Cirque produced four  $^{10}\text{Be}$  exposure ages of  $12.9 \pm 0.7$  ka (Med-1),  $11.3 \pm 0.6$  ka (Med-2),  $13.5 \pm 0.8$  ka (Med-3), and  $12.4 \pm 0.8$  ka (Med-4) (mean-weighted age:  $12.5 \pm 0.8$  ka; Fig. 56.5; Jomelli et al., 2020). With a SCF of 0.91, the ages for those samples change to  $13.5 \pm 2.2$  ka (Med-1),  $13.6 \pm 1.5$  ka (Med-2),  $13.6 \pm 1.5$  ka (Med-3) and  $13.6 \pm 1.5$  ka (Med-4) (mean weighted age:  $13.2 \pm 0.9$  ka; remodeled by Reixach et al., 2021). These recalculated ages show that Médecourbe Cirque hosted a small glacier (1.6 km long, descending to  $\sim 2230$  m) during the B-A and onset of the YD. Reconstructed glaciological and palaeoclimatic conditions indicate an ELA at 2525 m, a mass-balance gradient of  $0.41 \pm 0.03 \text{ m}\cdot\text{yr}^{-1}\cdot 100 \text{ m}^{-1}$ , and best-fitting P and T pairs of  $-60 \pm 7\%$  and  $-7.0 \pm 0.5$  °C, respectively. The position of Médecourbe Cirque is relatively sheltered by the Bassiès massif from Atlantic weather systems entering from the NW, which explains the sharp offset in ELA between the coeval Médecourbe and Mouscadous glaciers (Reixach et al., 2021).

In the upper Ariège valley, the presence of a glacier in the Pas de la Casa area during the YD is entirely plausible, but this hypothesis currently lacks conclusive age constraints from ice-marginal deposits—whether from the Hospitalet stadial moraines further down, or among the cirques further up the valley. The best constraints come from remodeled exposure ages obtained from Orri Cirque at Col de Puymorens. Values show that the last glacier to be hosted by that valley (glacier front reaching the 2100 m elevation contour) was recorded during the B-A Interstadial (GI-1), and not during the YD (GS-1) as initially inferred by Pallàs et al. (2010). Likewise, on the south-facing flanks of massifs in the area, the last glaciers vanished during the B-A (GI-1). This scenario can be reconstructed by extrapolating to these south-facing cirques the rise in ELA obtained from robust constraints in the upper Ariège valley (+270 m between GS-2.1a and GI-1) and the Bassiès massif (+200 m between GS-2.1a and GI-1). This simulation reveals that accumulation zones on south-facing mountain flanks dwindle to vanishingly small sizes, implying not only that all the valley heads of the Tossa Plana and Campcardós massifs became deglaciated during the B-A (required ELA of 2700 m), but also that promoting a re-expansion of glaciers during the YD was unattainable (the potential ELA would have descended to 2650 m on the south flanks of Tossa Plana and Campcardós, both flat-topped mountains rising to maximum elevations of 2900 m). This reconstruction is fully compatible with the formation of rock glaciers in most south-facing cirques during the B-A Interstadial, continuing potentially also during the YD and linked to paraglacial readjustments of the slope system (Delmas et al., 2008; Palacios et al., 2015a; Andrés et al., 2018). The only exception detected so far is the SE-facing Grave Cirque (Carlit massif), which may have maintained a glacier up to 2 km in length during the B-A, and perhaps the YD, by reason of its exposure to abundant snow supply from Atlantic weather systems penetrating through a topographic saddle in the valley-head ridge (exposure age at  $12.6 \pm 2.7$  ka on a glacially-polished bedrock step at 2380 m,  $12.1 \pm 2.6$  ka without applying a SCF, Fig. 56.5, Delmas et al., 2022b).

### **56.3. Synthesis and conclusions**

Despite the uncertainties around existing bedrock or boulder exposure ages, mostly explained by uncertainties concerning snow shielding magnitudes at high elevations, it remains clear that the cold spike of the YD in the Pyrenees was sharp enough to entail a standstill, and locally even a readvance, of glacier fronts. These glaciers were nonetheless consistently confined to the cirques, and (depending on local topoclimatic conditions) their lengths never exceeded 3–6 km. As a result, it is unlikely that ELAs reconstructed locally on that basis can be confidently extrapolated to the entire mountain range and be granted regional significance (Table 56.1).

Deglaciation favoured intense paraglacial readjustments on cirque headwalls and valley sides. During the YD, this promoted the development of rock glaciers within glacial cirques (García-Ruiz et al., 2016) as well as the formation of debris-covered glaciers in some cirques with abundant debris supply from the headwalls (Oliva et al., 2021). Some of these features remained active throughout the YD until the early Holocene because of thick debris mantles insulating the underlying permafrost and relict ice masses. Any residual ice finally melted away during the Holocene Thermal Maximum (Oliva et al., 2021).

## References

- Andrés, N., Gómez-Ortiz, A., Fernández-Fernández, J.M., Tanarro, L.M., Salvador-Franch, F., Oliva, M., Palacios, D., 2018. Timing of deglaciation and rock glacier origin in the southeastern Pyrenees: a review and new data. *Boreas* 47, 1050–1071.
- Bartolomé, M., Moreno, A., Sancho, C., Stoll, H.M., Cacho, I., Spötl, C., Belmonte, A., Edwards, R.L., Cheng, H., Hellstrom, J.C., 2015. Hydrological change in southern Europe responding to increasing North Atlantic overturning during Greenland Stadial 1. *Proceedings of the National Academy of Sciences* 112, 6568–6572.
- Bernal-Wormull, J.L., Moreno, A., Bartolomé, M., Aranburu, A., Arriolabengoa, M., Iriarte, E., Cacho, I., Spötl, C., Edwards, R.L., Cheng, H., 2021. Immediate temperature response in northern Iberia to last deglacial changes in the North Atlantic. *Geology* 49, 999–1003.
- Cacho, I., Grimalt, J.O., Pelejero, C., Canals, M., Sierro, F.J., Flores, J.A., Shackleton, N., 1999. Dansgaard-Oeschger and Heinrich event imprints in Alboran Sea paleotemperatures. *Paleoceanography* 14, 698–705.
- Cacho, I., Grimalt, J.O., Canals, M., Saffi, L., Shackleton, N.J., Schönfeld, J., Zahn, R., 2001. Variability of the Western Mediterranean sea surface temperature during the last 25,000 years and its connection with the Northern Hemisphere climatic changes. *Paleoceanography* 16, 40–52.
- Cacho, I., Grimalt, O., Canals, M., 2002. Response of the Western Mediterranean Sea to rapid climatic variability during the last 50,000 years: a molecular biomarker approach. *Journal of Marine Systems* 33–34, 253–272.
- Crest, Y., Delmas, M., Braucher, R., Gunnell, Y., M., Calvet, M., 2017. Cirques have growth spurts during deglacial and interglacial periods: Evidence from  $^{10}\text{Be}$  and  $^{26}\text{Al}$  nuclide inventories in the central and eastern Pyrenees. *Geomorphology* 278, 60–77.
- Delmas, M., Gunnell, Y., Braucher, R., Calvet, M., Bourlès, D. 2008. Exposure age chronology of the last glacial cycle in the eastern Pyrenees. *Quaternary Research* 69, 231–241.

Delmas, M., Calvet, M., Gunnell, Y., Braucher, R., Bourlès, D., 2011. Palaeogeography and  $^{10}\text{Be}$  exposure chronology of Middle and Late Pleistocene glacier systems in the northern Pyrenees: implications for reconstructing regional palaeoclimates. *Palaeogeography, Palaeoclimatology, Palaeoecology* 305, 109–122.

Delmas, M., Braucher, R., Gunnell, Y., Guillou, V., Calvet, M., Bourlès, D., 2015. Constraints on Pleistocene glaciofluvial terrace age and related soil chronosequence features from vertical  $^{10}\text{Be}$  profiles in the Ariège River catchment (Pyrenees, France). *Global and Planetary Change* 132, 39–53.

Delmas, M., Calvet, M., Gunnell, Y., Voinchet, P., Manel, C., Braucher, R., Tissoux, H., Bahain, J.J., Perrenoud, C., Saos, T., 2018. Terrestrial  $^{10}\text{Be}$  and Electron Spin Resonance dating of fluvial terraces quantifies Quaternary surface uplift in the eastern Pyrenees. *Quaternary Science Reviews* 193, 188–211.

Delmas, M., Gunnell, Y., Calvet, M., Reixach, T., Oliva, M., 2022a. The Pyrenees: environments and landforms in the aftermath of the LGM (18.9–14.6 ka). In: Palacios, D., Hughes, P., García-Ruiz, J.M., Andrés, A. (Eds.), *European Glacial Landscapes: Maximum Extent of Glaciations*. Elsevier (in press).

Delmas, M., Oliva, M., Gunnell, Y., Fernandes, M., Reixach, T., Fernández-Fernández, J.M., Calvet, M., 2022b. The Pyrenees: glacial landforms from the Bølling–Allerød Interstadial (14.6–12.9 ka). In: Palacios, D., Hughes, P., García-Ruiz, J.M., Andrés, A. (Eds.), *European Glacial Landscapes: Maximum Extent of Glaciations*. Elsevier (in press).

Delmas, M., 2019. L'apport des nucléides cosmogéniques produits in situ à la quantification multi-échelle des changements environnementaux quaternaires dans les montagnes des latitudes tempérées. Mémoire d'Habilitation à Diriger des Recherches, Université Lumière Lyon 2, 312 p.

Fernandes, M., Oliva, M., Vieira, G., Palacios, D., Fernández-Fernández, J.M., Garcia-Oteyza, J., Schimmelpfennig, I., Team, A., Antoniades, D., 2021. Glacial oscillations during the Bølling–Allerød Interstadial–Younger Dryas transition in the Ruda Valley, central Pyrenees. *Journal of Quaternary Science*, 1–17, <https://doi.org/10.1002/jqs.3379>.

García-Ruiz, J.M., Palacios, D., González-Sampériz, P., de Andrés, N., Moreno, A., Valero-Garcés, B., Gómez-Villar, A., 2016. Mountain glacier evolution in the Iberian Peninsula during the Younger Dryas. *Quaternary Science Reviews* 138, 16–30.

García-Ruiz, J.M., Palacios, D., Hughes, Ph., 2022. Concept and global context of the glacial landforms from Younger Dryas (chapter 46). In: Palacios, D., Hughes, P., García-Ruiz, J.M., Andrés, A. (Eds.), *European Glacial Landscapes: Maximum Extent of Glaciations*. Elsevier (in press).

González-Sampériz, P., Valero-Garcés, B.L., Moreno, A., Jalut, G., García-Ruiz, J.M., Martí-Bono, C., Delgado-Huertas, A., Navas, A., Otto, T., Dedoubat, J.J., 2006. Climate variability in the Spanish Pyrenees during the last 30,000 yr revealed by the El Portalet sequence. *Quaternary Research* 66, 38–52.

Fletcher, W.J., Sánchez Goñi, M.F., Allen, J.R.M., Cheddadi, R., Combourieu-Nebout, N., Huntley, B., Lawson, I., Londeix, L., Magri, D., Margari, V., Müller, U.C., Naughton, F., Novenko, E., Roucoux, K., Tzedakis, P.C., 2009. Millennial-scale variability during the last glacial in vegetation records. *Quaternary Science Reviews* 29, 2839–2864.

González-Sampériz, P., Valero-Garcés, B., Carrión, J.S., 2004. Was de Ebro Valley a refugium for temperate trees? *Anales de Biología* 26, 13–20.

- Jalut, G., Montserrat Marti, J., Fontugne, M., Delibrias, G., Vilaplana, J.M., Julia, R., 1992. Glacial to Interglacial vegetation changes in the northern and southern Pyrenees: deglaciation, vegetation cover and chronology. *Quaternary Science Reviews* 11, 449–480.
- Jomelli, V., Chapron, E., Favier, V., Rinterknecht, V., Braucher, R., Tournier, N., Gascoïn, S., Marti, R., Galop, D., Binet, S., Deschamps-Berger, C., Tissoux, H., Aumaître, G., Bourlès, D.L., Keddadouche, K., 2020. Glacier fluctuations during the Late Glacial and Holocene on the Ariège valley, northern slope of the Pyrenees and reconstructed climatic conditions. *Mediterranean Geoscience Reviews* 2, 37–51.
- Melki, T., Kallel, N., Jorissen, F.J., Guichard, F., Dennielou, B., Berné, S., Labeyrie, L., Fontugne, M., 2009. Abrupt climate change, sea surface salinity and paleoproductivity in the western Mediterranean Sea (Gulf of Lion) during the last 28 kyr. *Palaeogeography, Palaeoclimatology, Palaeoecology* 279, 96–113.
- Millet, L., Rius, D., Galop, D., Heiri, O., Brooks, S.J., 2012. Chironomid-based reconstruction of Late-Glacial summer temperatures from the Ech palaeolake record (French western Pyrenees). *Palaeogeography, Palaeoclimatology, Palaeoecology* 315, 86–99.
- Morellón, M., Valero-Garcés, B., Vegas-Villarrúbia, T., González-Sampériz, P., Romero, O., Delgado-Huertas, A., Mata, P., Moreno, A., Rico, M., Corella, J.P., 2009. Lateglacial and Holocene palaeohydrology in the western Mediterranean region: the Lake Estanya record (NE Spain). *Quaternary Science Reviews* 28, 2582–2599.
- Moreno, A., González-Sampériz, P., Morellón, M., Valero-Garcés, B.L., Fletcher, W.J., 2012. Northern Iberian abrupt climate change dynamics during the last glacial cycle: a view from lacustrine sediments. *Quaternary Science Reviews* 36, 139–153.
- Moreno, A., Svensson, A., Brooks, S.J., Connor, S., Engels, S., Fletcher, W., Genty, D., Heiri, O., Labuhn, I., Persoiu, A., Peyron, O., Sadori, L., Valero-Garcés, B., Wulf, S., Zanchetta G., 2014. A compilation of Western European terrestrial records 60–8 ka BP: towards an understanding of latitudinal climatic gradients. *Quaternary Science Reviews* 106, 167–185.
- Mouchéné, M., van der Beek, P., Mouthereau, F., Carcaillet, J., 2017. Controls on Quaternary incision of the Northern Pyrenean foreland: Chronological and geomorphological constraints from the Lannemezan megafan, SW France. *Geomorphology* 281, 78–93.
- Muñoz Sobrino, C., Heiri, O., Hazekamp, M., van der Velden, D., Kirilova, E.P., García-Moreiras, I., Lotter, A.F., 2013. New data of the Lateglacial period of SW Europe: a high-resolution multiproxy record from Laguna de La Roya (NW Iberia). *Quaternary Science Reviews* 80, 58–77.
- Naughton, F., Toucanne, S., Landais, A., Rodrigues, T., Vazquez Riveiros, N., Sánchez Goñi, M.F., 2022. The Younger Dryas (chapter 7). In: Palacios, D., Hughes, P., García-Ruiz, J.M., Andrés, A. (Eds.), *European Glacial Landscapes: Maximum Extent of Glaciations*. Elsevier (in press).
- Nivière, B., Lacan, P., Regard, V., Delmas, M., Calvet, M., Huyghe, D., Roddaz, B., 2016. Evolution of the late Pleistocene Aspe River (Western Pyrenees, France). Signature of climatic events and active tectonics. *Compte Rendus Géoscience* 348, 203–212.
- Oliva, M., Palacios, D., Fernández-Fernández, J.M., Rodríguez-Rodríguez, L., García-Ruiz, J.M.M., Andrés, N., Carrasco, R.M.M., Pedraza, J., Pérez-Alberti, A., Valcárcel, M., Hughes, P.D.D., 2019. Late Quaternary glacial phases in the Iberian Peninsula. *Earth-Science Reviews* 192, 564–600.

Oliva, M., Fernandes, M., Palacios, D., Fernández-Fernández, J.M., Schimmelpfennig, I., Team, A.S.T.E.R., Antoniadou, D., 2021. Rapid deglaciation during the Bølling-Allerød Interstadial in the Central Pyrenees and associated glacial and periglacial landforms. *Geomorphology* 385, 107735.

Palacios, D., Gómez-Ortiz, A., de Andrés, N., Vázquez-Selem, L., Salvador-Franch, F., Oliva, M. 2015a. Maximum Extent of Late Pleistocene Glaciers and Last Deglaciation of La Cerdanya Mountains, Southeastern Pyrenees. *Geomorphology* 231, 116–129.

Palacios, D., de Andrés, N., López-Moreno, J.I., García-Ruiz, J.M. 2015b. Late Pleistocene deglaciation in the central Pyrenees: the upper Gállego valley. *Quaternary Research* 83, 397–414.

Palacios, D., García-Ruiz, J.M., Andrés, N., Schimmelpfennig, I., Campos, N., Léanni, L., ASTER Team, 2017. Deglaciation in the central Pyrenees during the Pleistocene-Holocene transition: timing and geomorphological significance. *Quaternary Science Reviews* 162, 111–127.

Palacios, D., 2022. Concept and global context of the glacial landforms from the Bølling-Allerød Interstadial. In: Palacios, D., Hughes, P., García-Ruiz, J.M., Andrés, A. (Eds.), *European Glacial Landscapes: Maximum Extent of Glaciations*. Elsevier (in press).

Pallàs, R., Rodés, A., Braucher, R., Carcaillet, J., Ortuño, M., Bordonau, J., Bourlès, D., Vilaplana, J.M., Masana, E., Santanach, P., 2006. Late Pleistocene and Holocene glaciation in the Pyrenees: a critical review and new evidence from <sup>10</sup>Be exposure ages, south-central Pyrenees. *Quaternary Science Reviews* 25, 2937–1963.

Pallàs, R., Rodés, A., Braucher, R., Bourlès, D., Delmas, M., Calvet, M., Gunnell, Y., 2010. Small, isolated glacial catchments as priority targets for cosmogenic surface exposure dating of Pleistocene climate fluctuations, southeastern Pyrenees. *Geology* 38, 891–894.

Rasmussen, S.O., Bigler, M., Blockley, S.P., Blunier, T., Buchardt, S.L., Clausen, H.B., Cvijanovic, I., Dahl-Jensen, D., Johnsen, S.J., Fischer, H., Gkinis, V., Guillevic, M., Hoek, W.Z., Lowe, J.J., Pedro, J.B., Popp, T., Seierstad, I.K., Steffensen, J.P., Svensson, A.M., Vallelonga, P., Vinther, B.M., Walker, M.J.C., Wheatley, J.J., Winstrup, M., 2014. A stratigraphic framework for abrupt climatic changes during the Last Glacial period based on three synchronized Greenland ice-core records: refining and extending the INTIMATE event stratigraphy. *Quaternary Science Reviews* 106, 14–28.

Reille, M., Andrieu, V., 1993. Variations de la limite supérieure des forêts dans les Pyrénées (France) pendant le Tardiglaciaire. *Compte rendu de l'Académie des Sciences de Paris Série II* 316, 547–551.

Reixach, T., Delmas, M., Braucher, R., Gunnell, Y., Mahé, C., Calvet, M. 2021. Climatic conditions between 19 and 12 ka in the eastern Pyrenees, and wider implications for atmospheric circulation patterns in Europe. *Quaternary Science Reviews* 260, 106923

Rodrigues, T., Grimalt, J.O., Abrantes, F., Naughton, F., Flores, J.A., 2010. The last glacial-interglacial transition (LGIT) in the western mid-latitudes of the North Atlantic: abrupt sea surface temperature change and sea level implications. *Quaternary Science Reviews* 29, 1853–1862.

Stange, K.M., Van Balen, R.T., Carcaillet, J., Vandenberghe, J., 2013. Terrace staircase development in the southern Pyrenees foreland: inferences from <sup>10</sup>Be terrace exposure ages at the Segre River. *Global and Planetary Change* 101, 97–112.

Stange, K.M., Van Balen, R.T., Kasse, C., Vandenberghe, J., Carcaillet, J., 2014. Linking morphology across the glaciofluvial interface: a  $^{10}\text{Be}$  supported chronology of glacier advances and terrace formation in the Garonne River, northern Pyrenees, France. *Geomorphology* 207, 71–95.